Multi-Axis Additive Manufacturing:

Support-free, Mechanical Strength & Motion Planning

Charlie C. L. Wang

Department of Mechanical, Aerospace and Civil Engineering
The University of Manchester

April 12, 2022

MANCHESTER 1824
The University of Manchester

Additive Manufacturing (3D Printing)

- Defined by ASTM as:
  - Process of joining materials to make objects from 3D model data, usually layer upon layer
- Different Types of AM:
  - Lasers: Stereolithography Apparatus (SLA), Selective Laser Sintering (SLS)
  - Nozzles: Fused Deposition Modeling (FDM)
  - Print-heads: Multi-jet Modeling (MJM), Binder-jet Printing (3DP)
  - Cutters: Laminated Object Modeling (LOM)
- Mainly used for Rapid Prototyping (Past)
- More and More used for 'Mass'-Production (Present)

2.5D / 3D Printing ? Pros. and Cons.

- Planar-layer-based material accumulation
  - Simplify the algorithms of motion-planning
  - Limited shape of models that can be support-free fabricated – i.e., support-structures in many cases
  - Relatively weak mechanical property between layer – especially at the regions with thin and small features

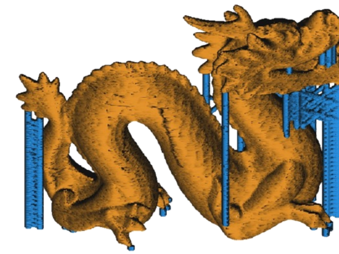

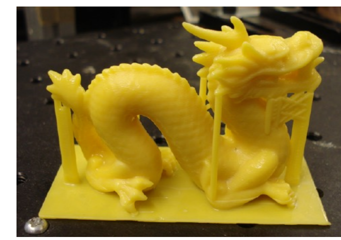

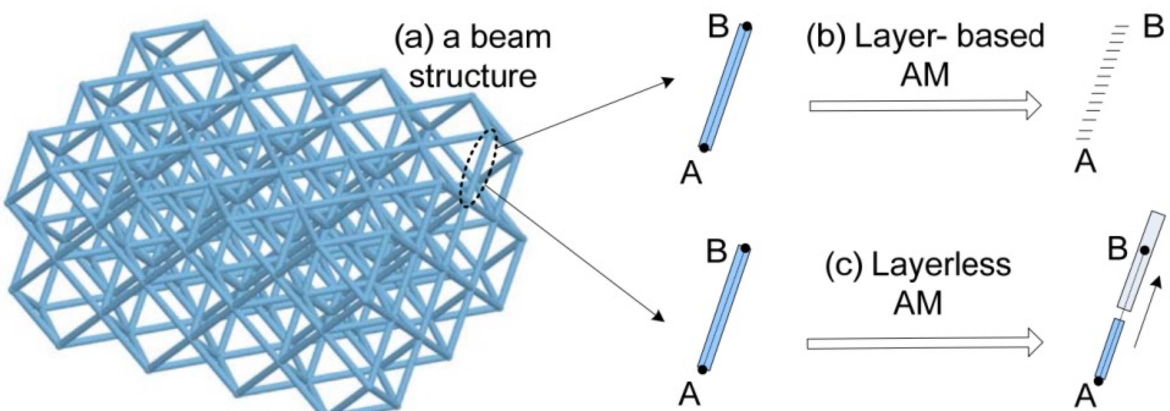

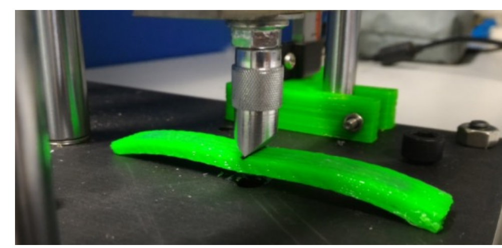

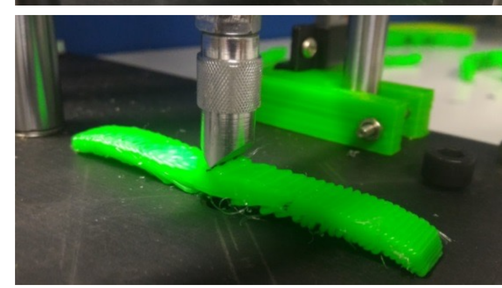

Robot-Assisted Additive Manufacturing: Multi-Axis and High-DOF Motion

- Using robot arms as device for motion control in AM
- Collaborative operations on two arms – More DoFs to fabricate curved regions / layers
- Challenges:
  - Slicing solid into curved surfaces
  - Collision-free tool path generation
  - Planning in Machine Coordinate Sys.

vs

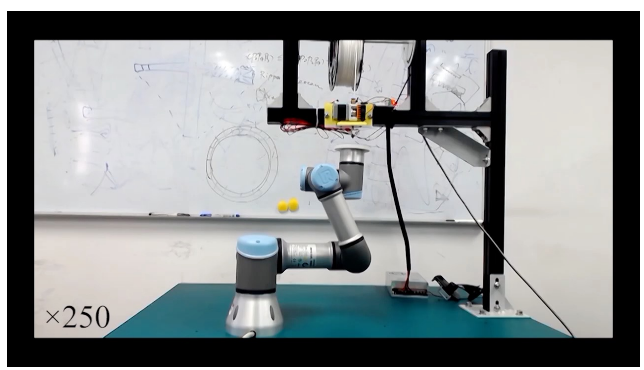

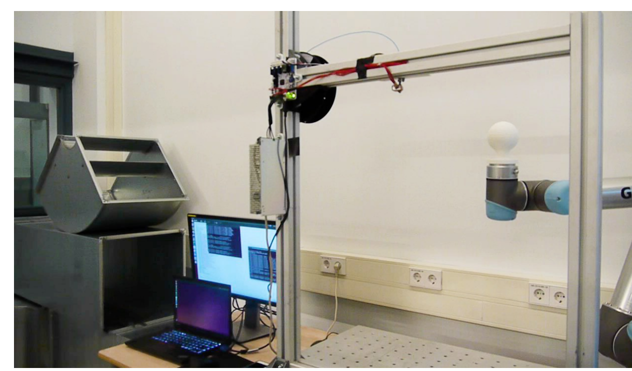

Chenming Wu, Chengkai Dai, Guoxin Fang, Yong-Jin Liu, and **Charlie C.L. Wang**, "RoboFDM: a robotic system for support-free fabrication using FDM", IEEE International Conference on Robotics and Automation (ICRA 2017).

Outline

- Support-free volume printing by multi-axis motion
- Multi-axis filament alignment with controlled anisotropic strength
- Motion Planning:
  - Planning jerk-optimized trajectory for redundant robots (robotic arm + position table)
  - Singularity-aware motion planning for multi-axis additive manufacturing (x-, y-, z-movement + tilting head / table)

Curved Support-Free Volume Printing

- Tool-path generation problem in volume is challenging:
  - Too many possibility of accumulating materials
  - How to plan collision-free motions for AM
- Problems of existing multi-axis AM approaches:
  - Only very simple shapes (i.e., not general for freeform models)
  - Build collision-detection into the loop of process planning (e.g., a sequence of 462k voxels – FCL takes ~3.4h in a fixed order)
  - When different orders are tested, much more time is needed

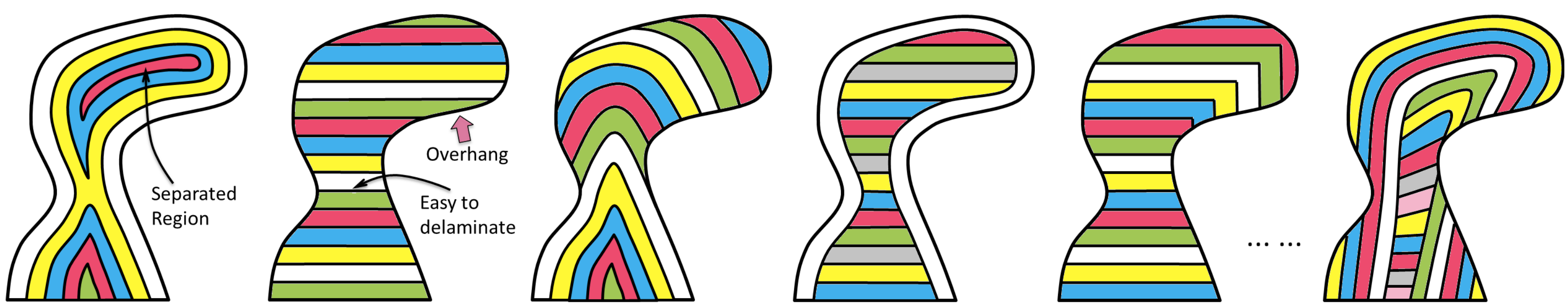

(a) Conformal structure (b) Planar layers as conventional (c) Semi-conformal Structure (d) Structure with less staircase artifacts (e) Support-free structure

Curved Support-Free Volume Printing

- **Our solution**: field-based method to decompose a solid into a sequence of collision-free working surfaces as curved layers, and then generate tool-paths on each layer
- Two levels of decomposition (constraints):
  - Volume-to-Surface – uniform, accessible & self-supported
  - Surface-to-Curve – uniform and continuous in position, orientation & pose

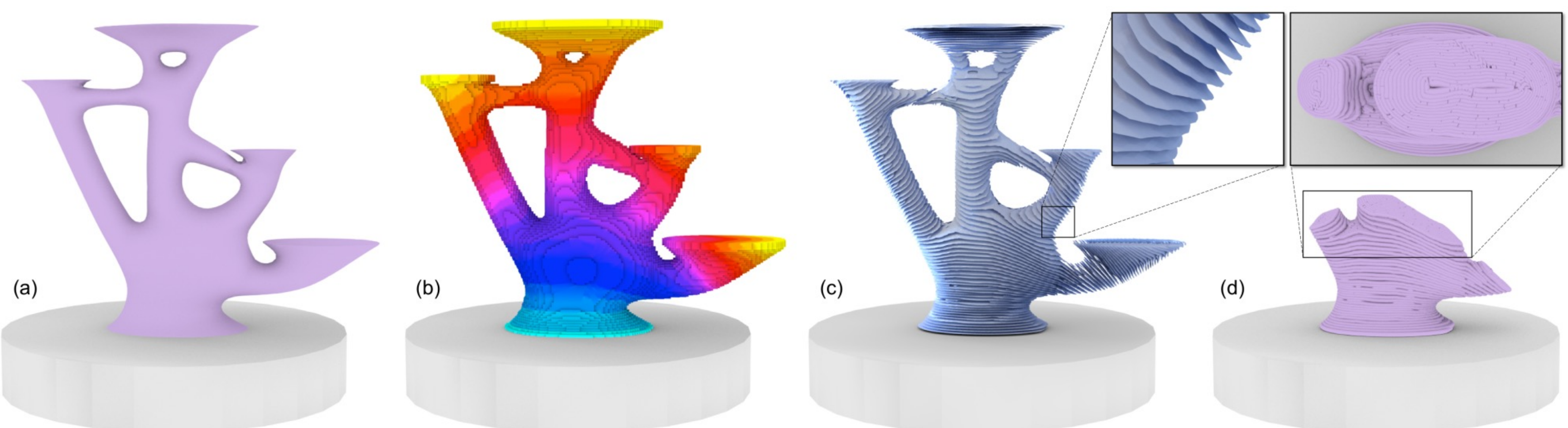

Video of Robotic 3D Printing

 C. Dai, **C.C.L. Wang**, C. Wu, S. Lefebvre, G. Fang, and Y.J. Liu, "Support-free Volume Printing by Multi-Axis Motion", *ACM Transactions on Graphics* (SIGGRAPH 2018), vol.37, no.4, article no.134 (13 pages), July 2018.

Pros. and Cons. of 2.5D Printing

- Planar-layer-based material accumulation
  - Simplify the algorithms of motion-planning
  - Limited shape of models that can be support-free fabricated – i.e., support-structures in many cases
  - Relatively weak mechanical property between layer – especially at the regions with thin and small features

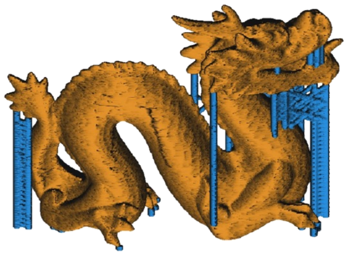

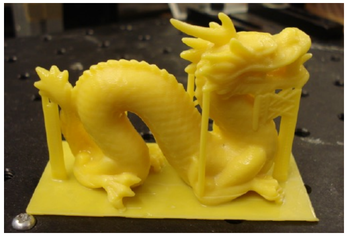

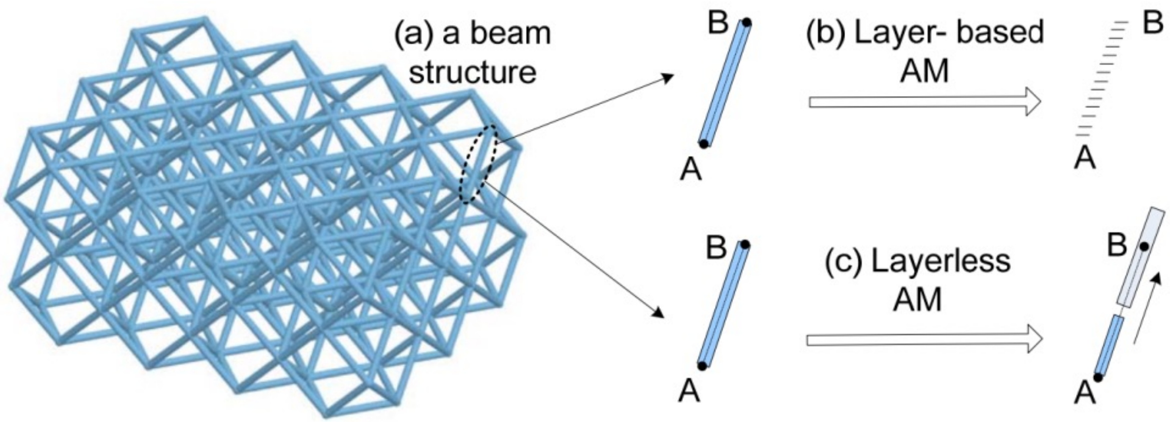

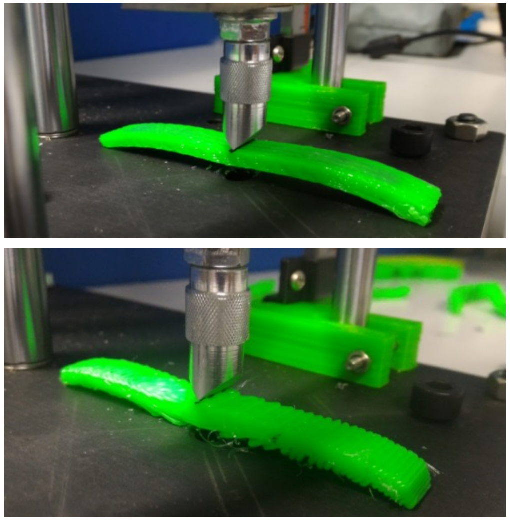

Outline

- Support-free volume printing by multi-axis motion
- Multi-axis filament alignment with controlled anisotropic strength
- Motion Planning:
  - Planning jerk-optimized trajectory for redundant robots (robotic arm + position table)
  - Singularity-aware motion planning for multi-axis additive manufacturing (x-, y-, z-movement + tilting head / table)

Anisotropy of Mechanical Property

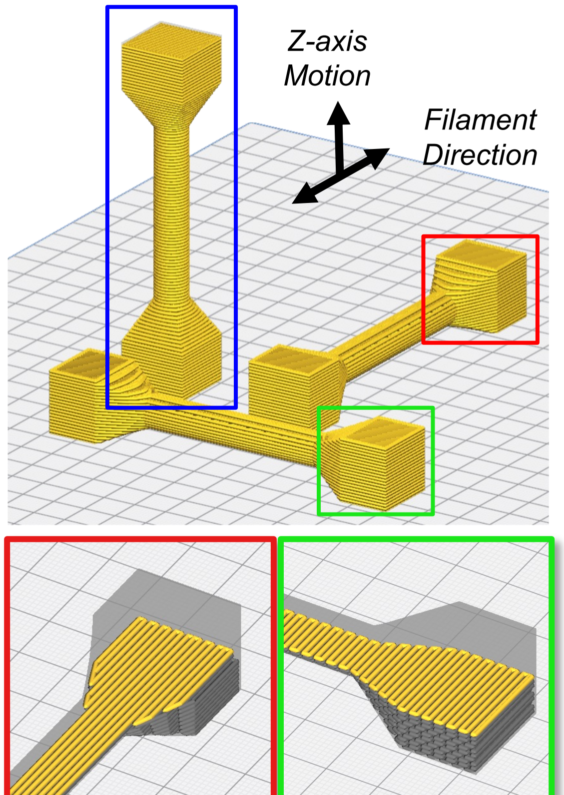

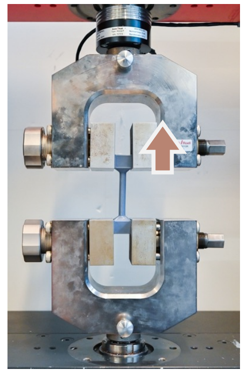

Tensile

Compress

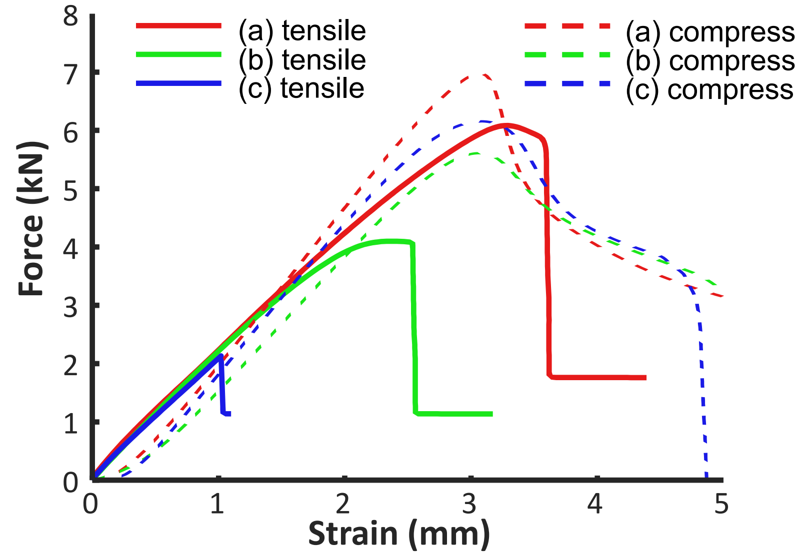

176% enhance in tensile test

27% enhance in compress test

[*Ahn et al, J. Rapid Prototyping. 2002; Tam and Muller, 3DP&AM. 2017*]

- Transversal direction is much weaker than axial direction
- Analyze the stress tensor distribution

Delamination: Major Source of Fracture

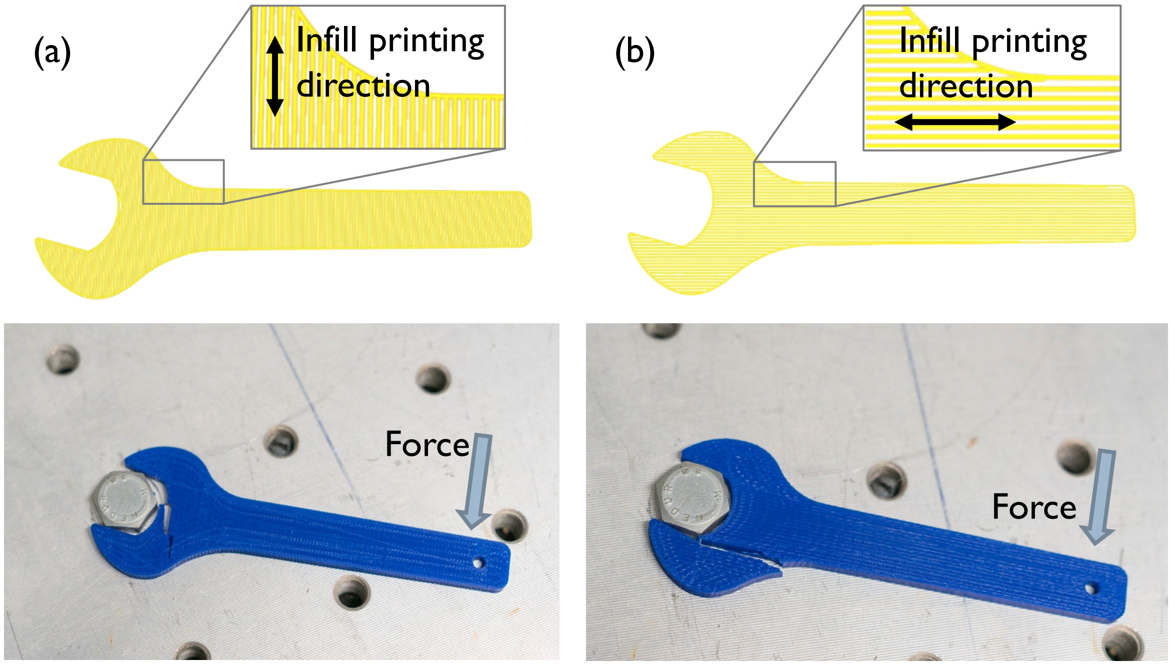

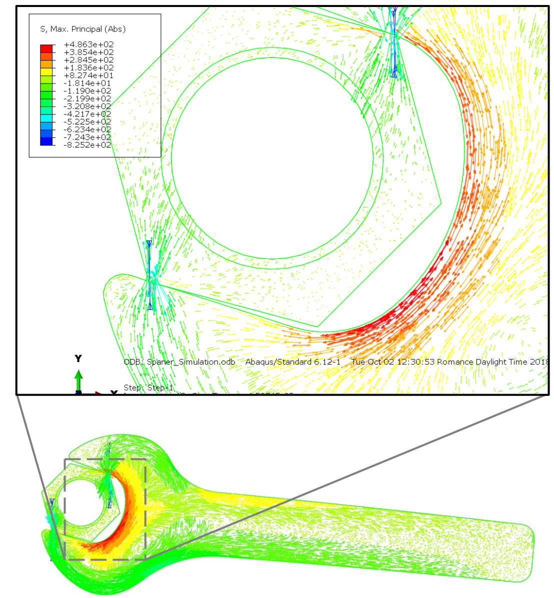

(c) Absolute maximum principal stress

- Anisotropic strength caused by the weak adhesion at incompletely filled area

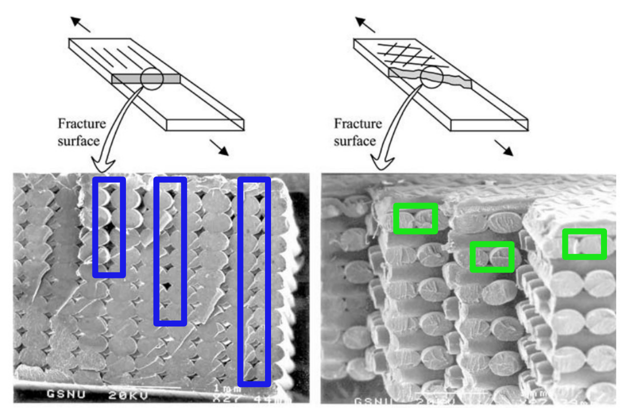

[*Ahn et al, J. Rapid Prototyping. 2002*]

Reinforcement by Filament Alignment

- **Our Solution:** aligning filaments along the directions of *principal stresses*
  - Slicing model with curved layers – be tangential to local principal stress direction
  - Generating toolpath in curved layers – following the vectors of principal stresses

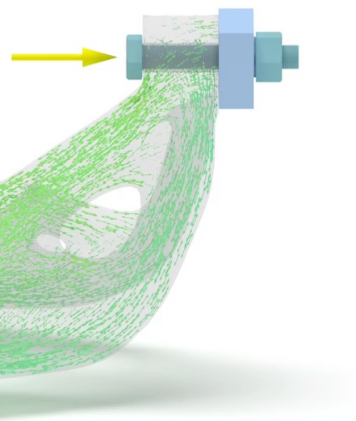

Computational Framework: Model Slicing by Optimized Scalar Field

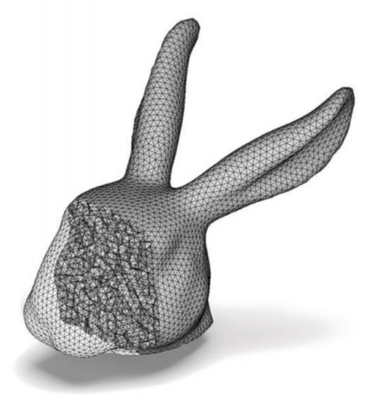

Model with volumetric mesh representation

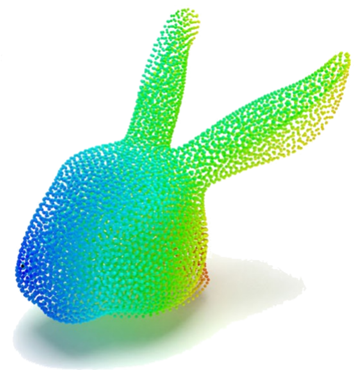

Optimized Scalar Field (on mesh vertex)

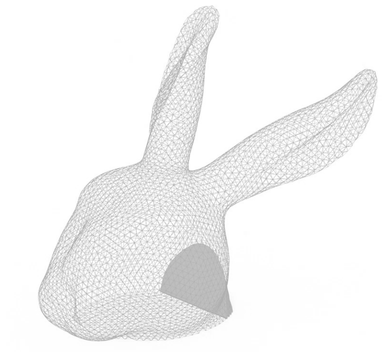

Iso-surfaces of Scalar Field as curved layers

- Computation is conducted on volumetric mesh:
  - Continuous representation (scalar field)
  - Effectively in integrating design & manufacturing objectives
    - Reinforcement (following the direction of principal stresses)
    - Fabrication constraints (smoothness, layer thickness control etc.)
  - Curved layers naturally fit with mesh boundary

Computational Framework: Design Objectives on Scalar Field (Gradient)

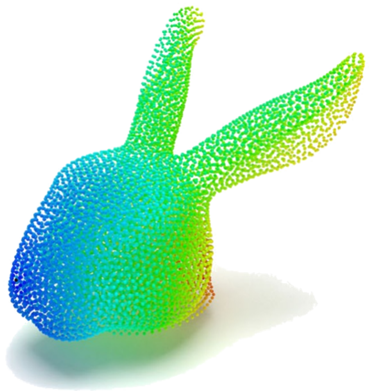

Piece-wise Linear Func.:

$$G^e(\mathbf{x}) = \sum_{i=1}^{4} \lambda_i(\mathbf{x}) g_i,$$

$$\nabla G^e(\mathbf{x}) = \left(\sum_{i=1}^{4} \frac{\partial \lambda_i(\mathbf{x})}{\partial x} g_i, \sum_{i=1}^{4} \frac{\partial \lambda_i(\mathbf{x})}{\partial y} g_i, \sum_{i=1}^{4} \frac{\partial \lambda_i(\mathbf{x})}{\partial z} g_i \right)$$
$$= \left(\sum_{i=1}^{4} a_i g_i, \sum_{i=1}^{4} b_i g_i, \sum_{i=1}^{4} c_i g_i \right).$$

Control growing direction - Reinforcement

Direction parallel to minimum principal stress direction

Principal Stress direction alignment

$$E_s = \sum_{e \in \mathcal{T}^*} V_e \|\nabla G(\mathbf{x}_e) \times \tau_{\min}(e)\|^2$$

Control growing speed

Ensure uniform layer thickness

Layer thickness constraint

$$E_t = \sum_{e \in \mathcal{T}} V_e (\|\nabla G(\mathbf{x}_e)\| - c)^2$$

Smoothness in curved layers

Harmonic of gradients

$$E_h = \sum_{(e_a, e_b) \in \mathcal{N}} A_{a,b} \|\nabla G(\mathbf{x}_{e_a}) - \nabla G(\mathbf{x}_{e_b})\|^2$$

Directly minimizing $w_s E_s + w_t E_t + w_h E_h$?

Computational Framework: Optimization on Vector Field

Layer thickness constraint

Apply normalization

$$\hat{\mathbf{v}}_e = c\mathbf{v}_e / \|\mathbf{v}_e\|$$

$$\Rightarrow \arg\min \sum_{e \in \mathcal{T}} w_e \|\nabla G(\mathbf{x}_e) - \hat{\mathbf{v}}_e\|^2$$

$$E_s = \sum_{e \in \mathcal{T}^*} V_e \|\nabla G(\mathbf{x}_e) \times \tau_{\min}(e)\|^2$$

$$E_t = \sum_{e \in \mathcal{T}} V_e (\|\nabla G(\mathbf{x}_e)\| - c)^2$$

$$E_h = \sum_{(e_a, e_b) \in \mathcal{N}} A_{a,b} \|\nabla G(\mathbf{x}_{e_a}) - \nabla G(\mathbf{x}_{e_b})\|^2$$

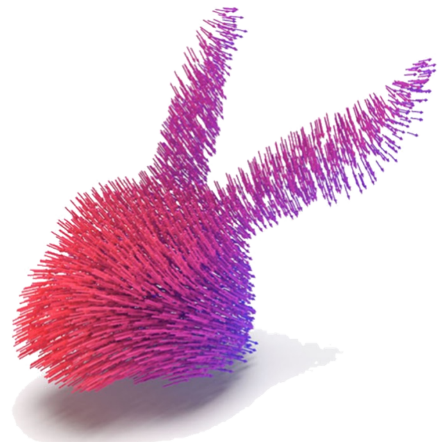

Vector Field V(·)

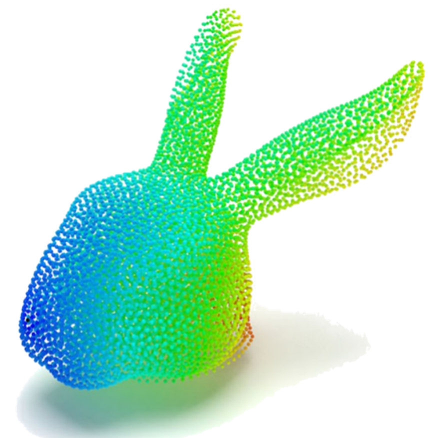

Optimized Scalar Field G(·)

Harmonic energy

$$\arg\min_{\mathbf{v}_e} E_w = \sum_{(e_a, e_b) \in \mathcal{N}} A_{a,b} \|\mathbf{v}_{e_a} - \mathbf{v}_{e_b}\|^2,$$

$$s.t. \quad \mathbf{v}_e = \rho_j \tau_{\min}(e) \quad (\forall e \in \mathcal{T}_j^*, j = 1, 2, \ldots m).$$

Stress-follow constraint

Harmonic of Gradients

Principal Stress direction alignment

Computational Framework: Toolpath Generation on Curved Layers

Projecting principal stresses on each layer

Vector Field

Scalar Field
Iso-curve as toolpath

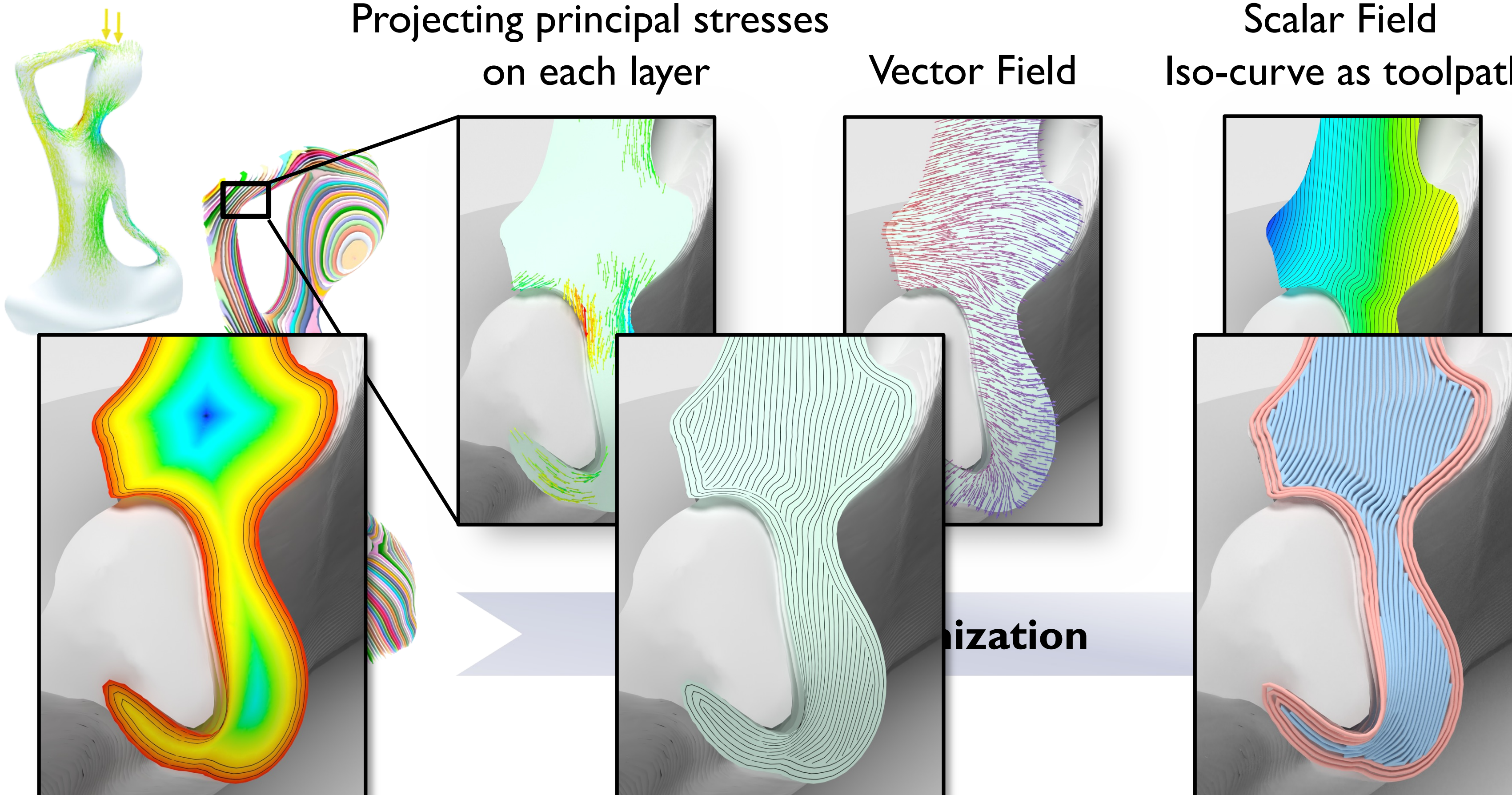

Contour-parallel toolpaths by boundary distance field

Combination of two types of toolpath

Final Connected toolpath

Computational Framework: Fabrication Enabling

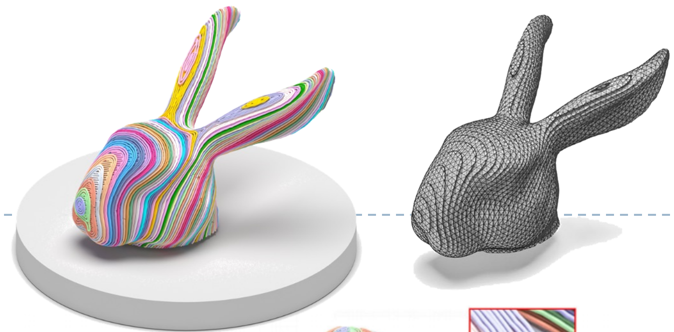

After generating curved layer / toolpath

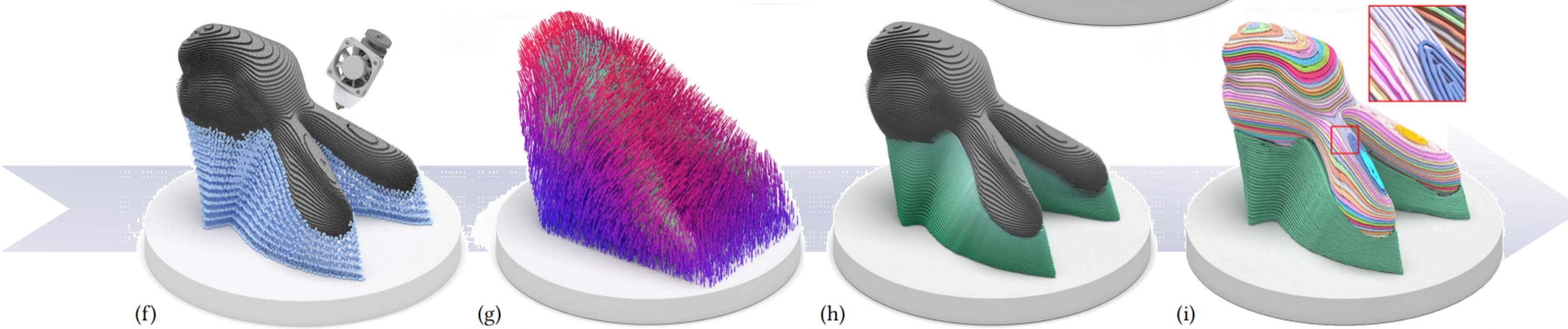

Find best printing direction
Detect overhang region

Field extrapolation for
support structure generation

Final layer + filament direction (with support)
Collision-free printing

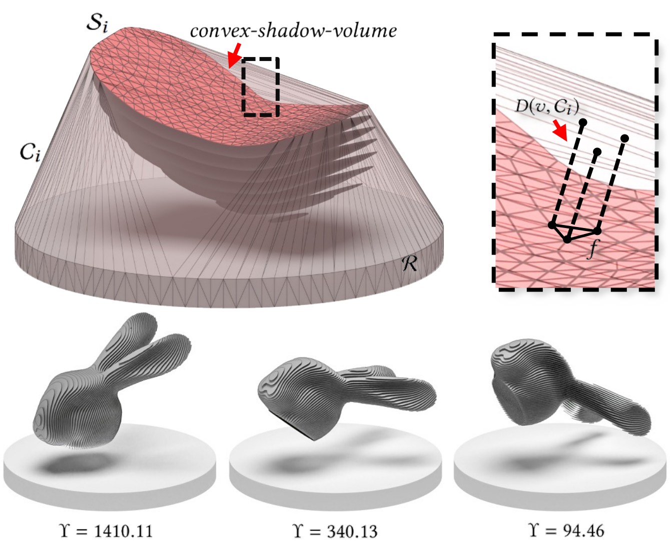

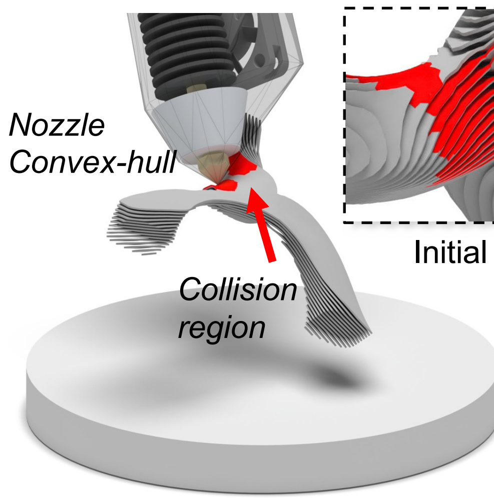

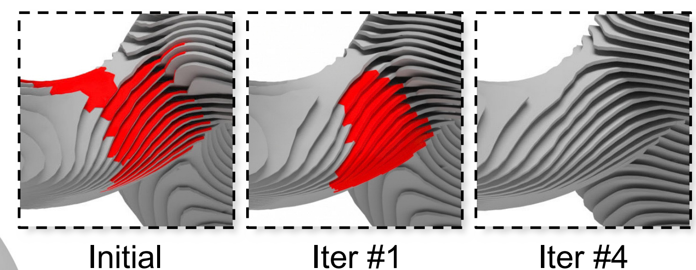

*Iteratively **flattening***
collision-region vector field

Minimizing Shadow Volume

Computational Results

Model	Fig.	Solid #tets	Time (sec.) of Field-Opt. Slicing: Field $\mathbf{v}(\cdot)$	Field $G(\cdot)$	Layers	Time (sec.) of Fabrication Enabling: Re-Ort.	Relax.†	Support‡	Slice⋆	Toolpath	Support #tets	Total (sec.)
Topo-opt	1	70,505	44.6	5.3	4.1	69.5	-	58.2	301.1	134.0	178.022	616.8
Bunny head	3	60,375	10.4	1.1	3.1	41.9	-	55.4	270.2	87.6	162,843	469.7
Yoga	4	52,446	28.4	3.6	3.5	124.2	-	84.5	523.2	100.9	142,183	868.3
C^2-model	7	46,547	18.6	2.4	5.8	71.1	21.3	78.6	218.2	37.5	152,799	453.5
Bridge	11	100,420	67.2	5.2	9.1	40.2	-	189.3	420.3	211.0	394,834	942.3

Computed with Intel (R) Core TM i7-9700K CPU (6 cores @ 3.6GHz) + 32GB RAM

- Field computing – *10%* of computing time
- Fabrication Enabling – *90%*
  (generate support structure
  and toolpath is time-consuming)
- All model within 15 mins

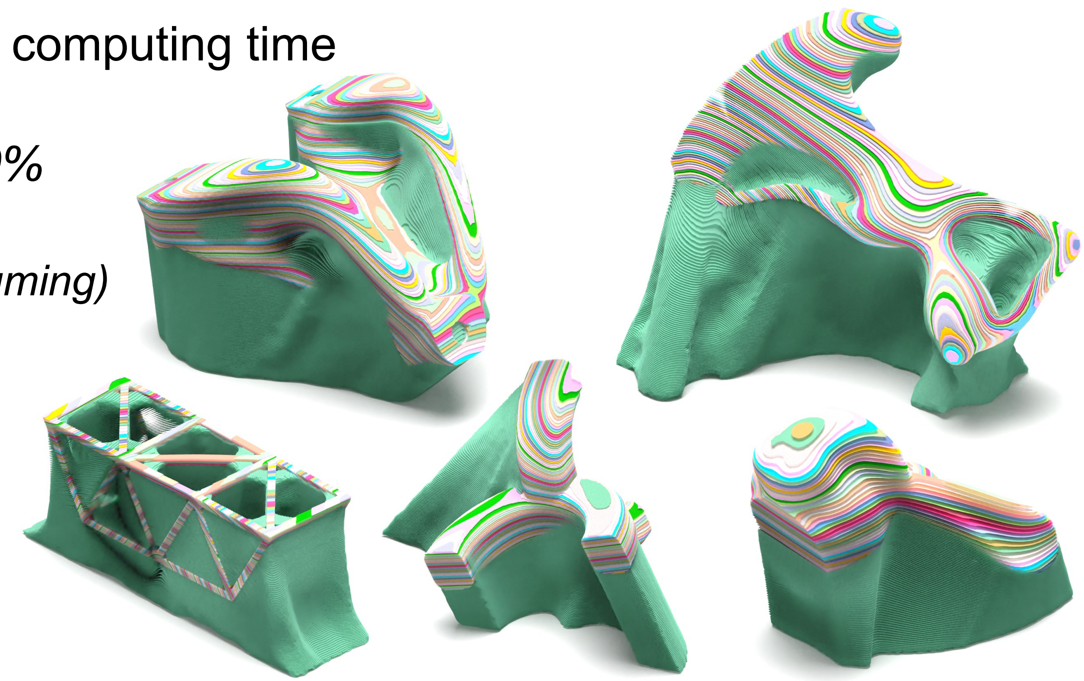

Hardware Setup for Fabrication

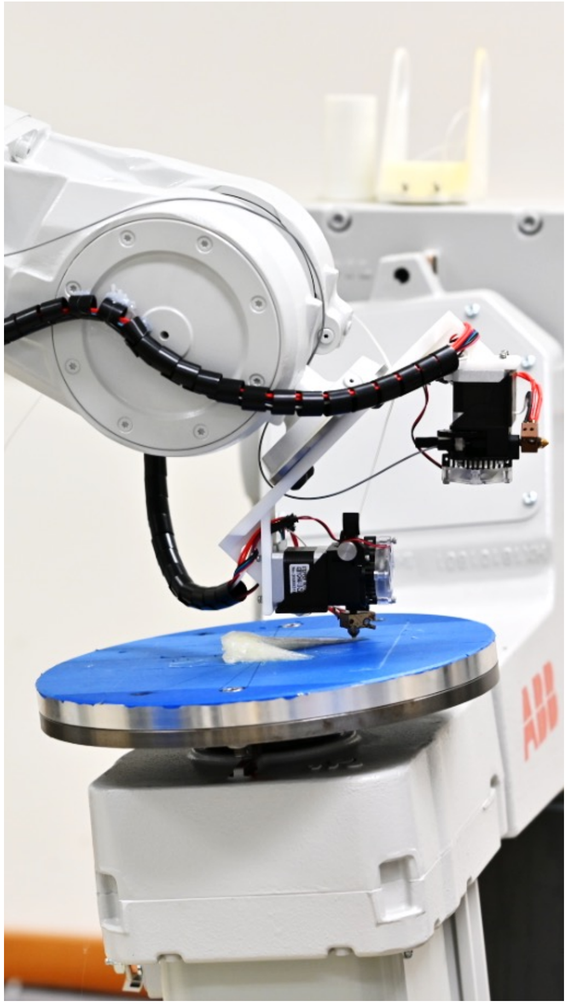

Setup 1 (5 DOFs):
Multi-axis parallel CNC machine

Setup 2 (8 DOFs):
Robot arm (ABB IRB 4600) + Position table

 G.Fang, T. Zhang, S. Zhong, X. Chen, Z. Zhong, and **C.C.L. Wang**, "Reinforced FDM: multi-axis filament alignment with controlled anisotropic strength", *ACM Transaction on Graphics* (SIGGRAPH Asia 2020), vol.39, no.6, article no.204, 2020.

Multi-Axis AM Fabrication

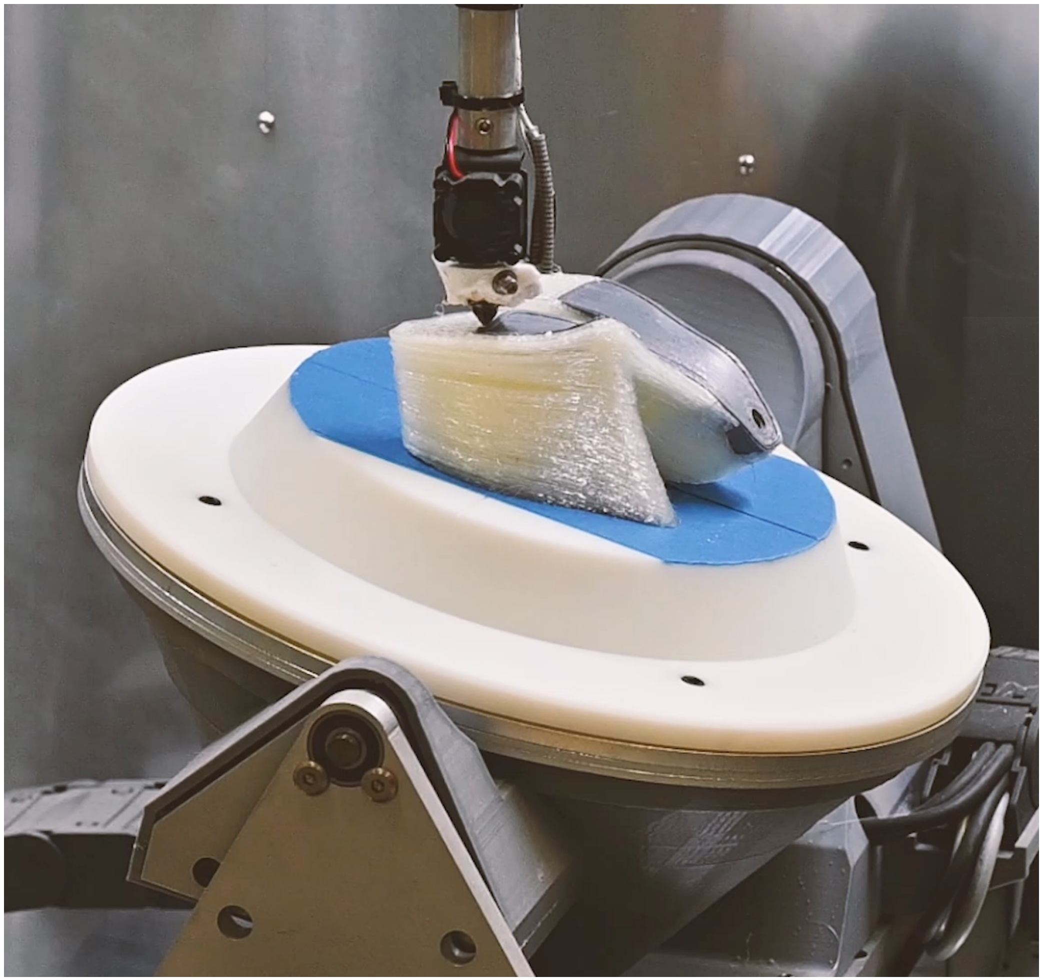

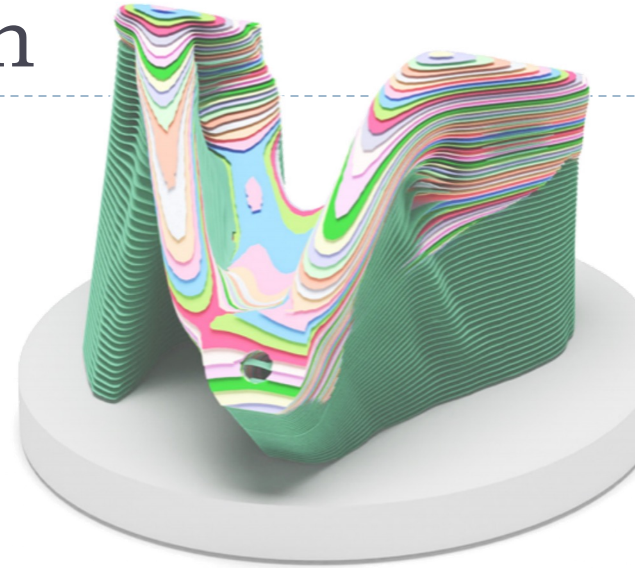

Fabricated result
(support structure removed)

G.Fang, T. Zhang, S. Zhong, X. Chen, Z. Zhong, and **C.C.L. Wang**, "Reinforced FDM: multi-axis filament alignment with controlled anisotropic strength", *ACM Transaction on Graphics* (SIGGRAPH Asia 2020), vol.39, no.6, article no.204, 2020.

Fabrication: Multi-Axis Parallel Machine

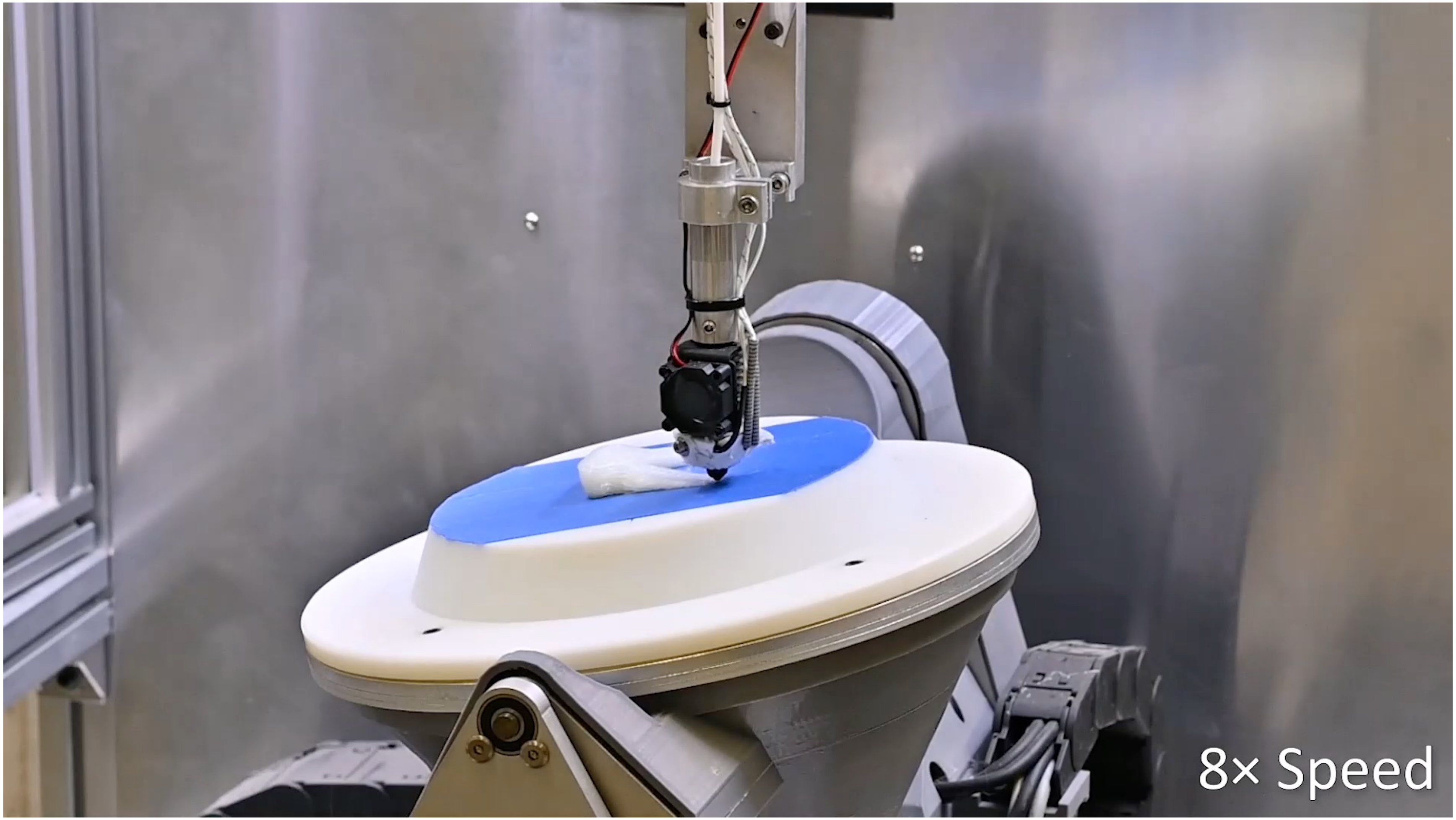

 G.Fang, T. Zhang, S. Zhong, X. Chen, Z. Zhong, and **C.C.L. Wang**, "Reinforced FDM: multi-axis filament alignment with controlled anisotropic strength", *ACM Transaction on Graphics* (SIGGRAPH Asia 2020), vol.39, no.6, article no.204, 2020.

Fabrication: Robotic Arm + Tilting Table

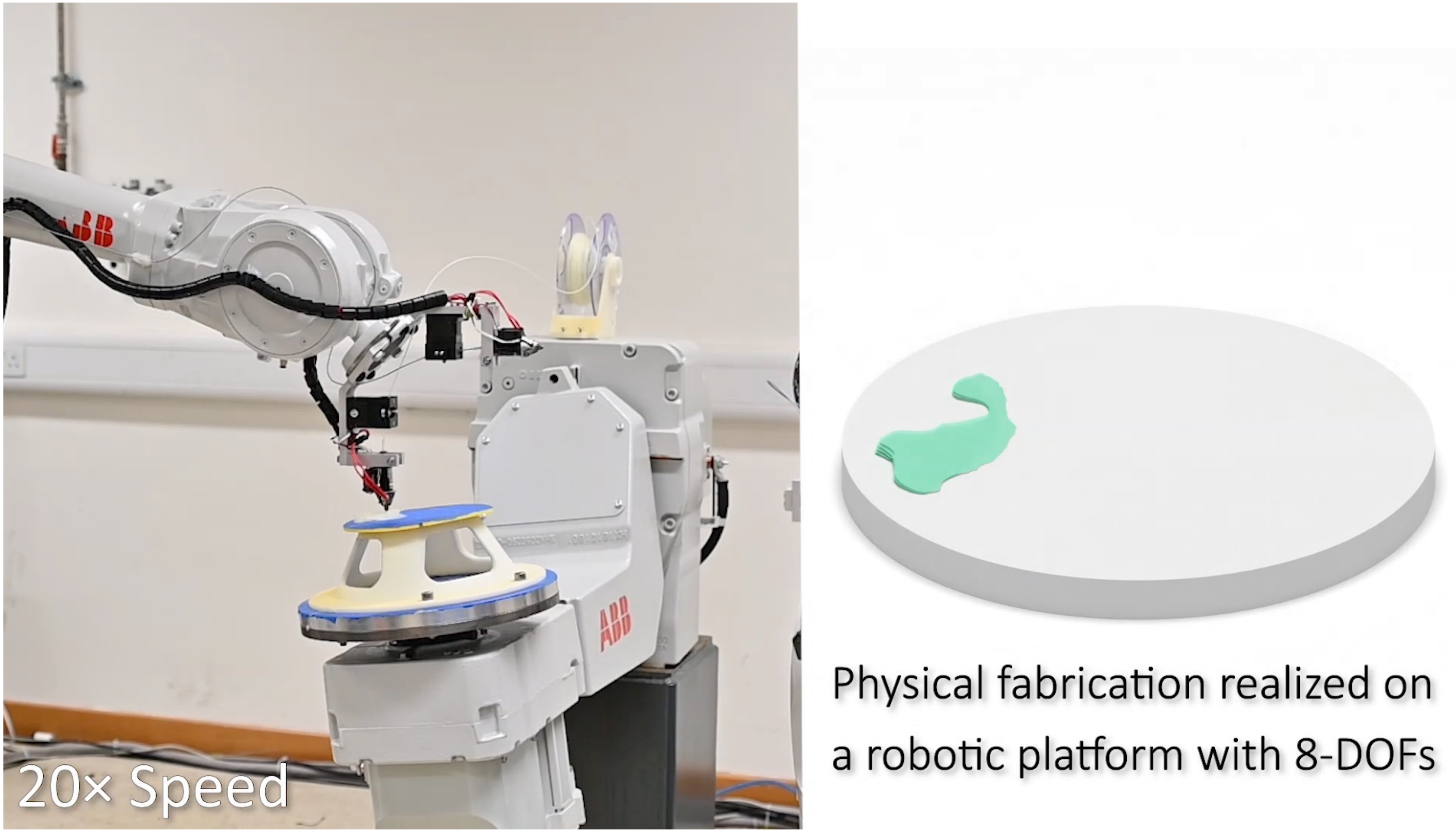

G.Fang, T. Zhang, S. Zhong, X. Chen, Z. Zhong, and **C.C.L. Wang**, "Reinforced FDM: multi-axis filament alignment with controlled anisotropic strength", *ACM Transaction on Graphics* (SIGGRAPH Asia 2020), vol.39, no.6, article no.204, 2020.

Reinforced FDM by Anisotropic Strength

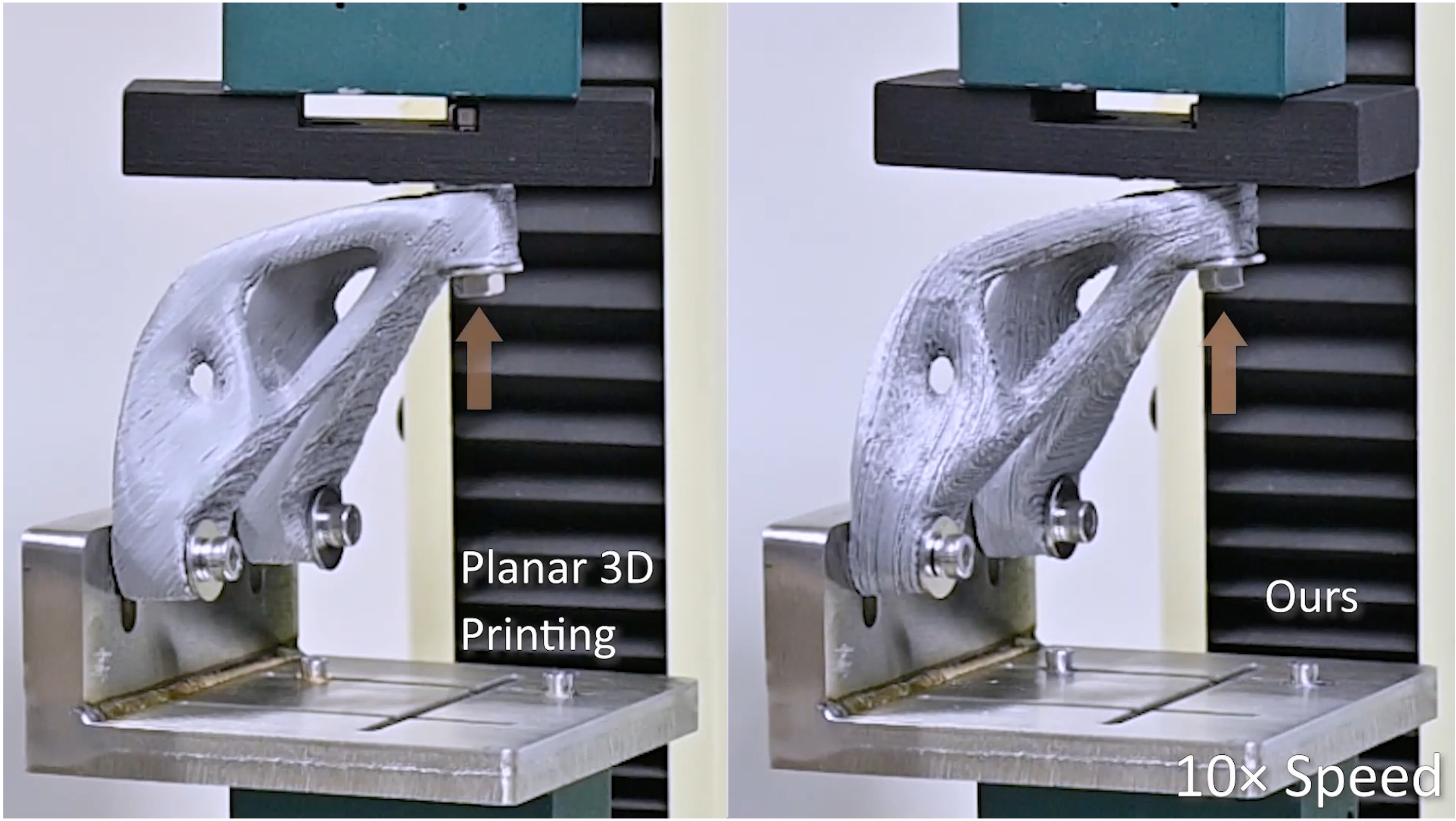

Stand up to 203% loads in breaking force

(compare to planar method with already optimized printing direction)

Validation: Physical Experiment

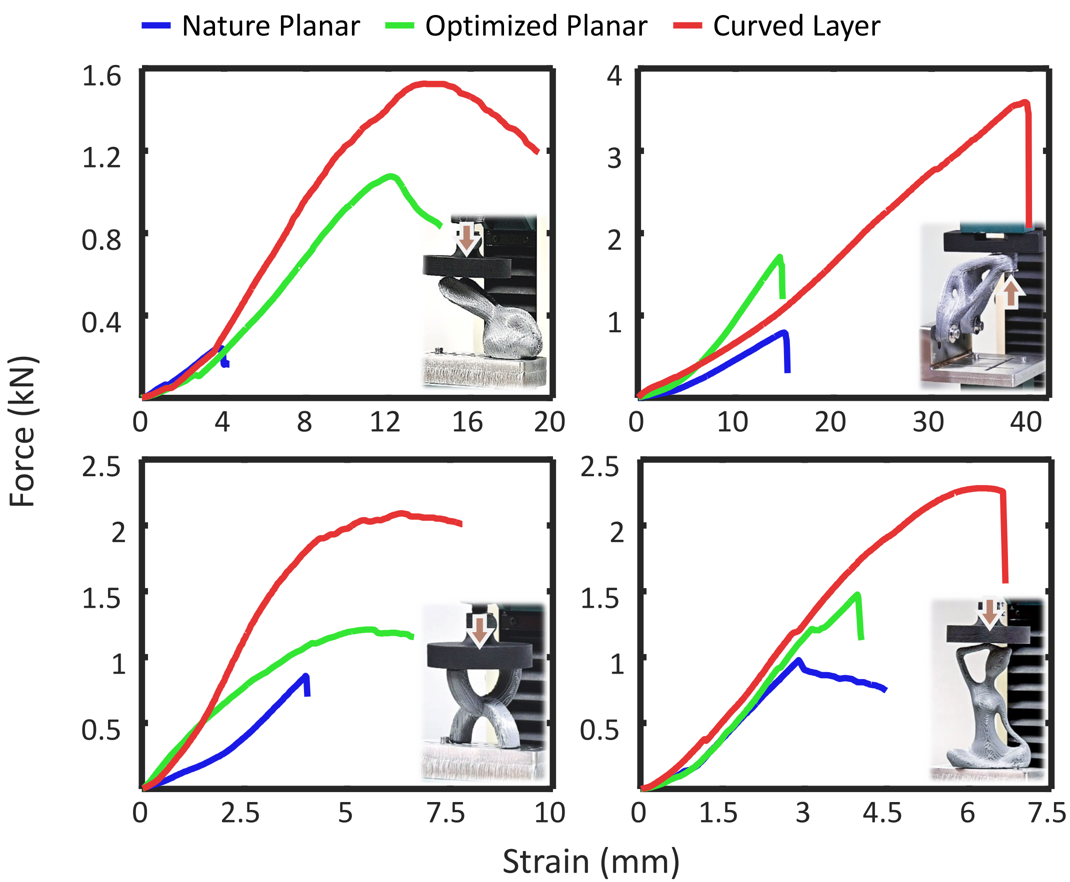

Bunny:
635% ↑ (natural ort.); 42% ↑ (optimized ort.)

Topo-opt:
450% ↑ (natural ort.); 103% ↑ (optimized ort.)

C^2-model:
243% ↑ (natural ort.); 73%↑ (optimized ort.)

Yoga:
132% ↑ (natural ort.); 55%↑ (optimized ort.)

G.Fang, T. Zhang, S. Zhong, X. Chen, Z. Zhong, and **C.C.L. Wang**, "Reinforced FDM: multi-axis filament alignment with controlled anisotropic strength", *ACM Transaction on Graphics* (SIGGRAPH Asia 2020), vol.39, no.6, article no.204, 2020.

Outline

- Support-free volume printing by multi-axis motion
- Multi-axis filament alignment with controlled anisotropic strength
- Motion Planning:
  - Planning jerk-optimized trajectory for redundant robots (robotic arm + position table)
  - Singularity-aware motion planning for multi-axis additive manufacturing (x-, y-, z-movement + tilting head / table)

Motivation

- Trajectory planning in MCS
- To realize complex motion
  - Multi-axis additive manufacturing
  - Tool-paths for freeform shape have many waypoints
  - Optimized performance in velocity, acceleration & jerk
- Kinematic redundancy is used to optimize motion
  - e.g., 6-DOF robotic arm for 5-DOF constrained tool-path

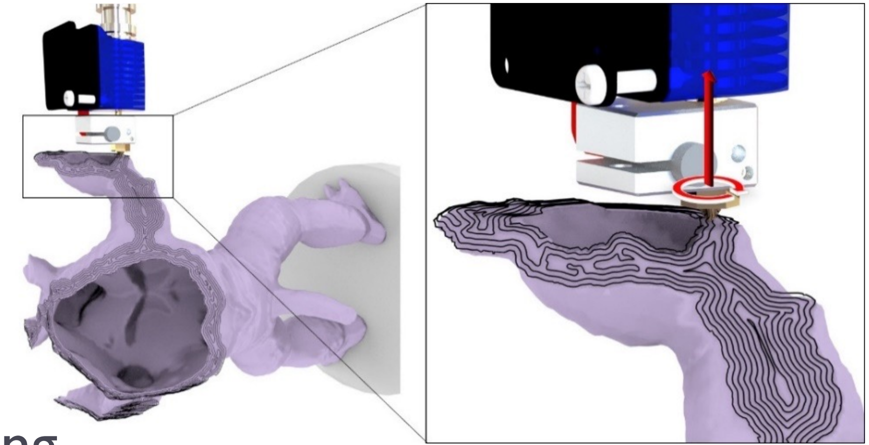

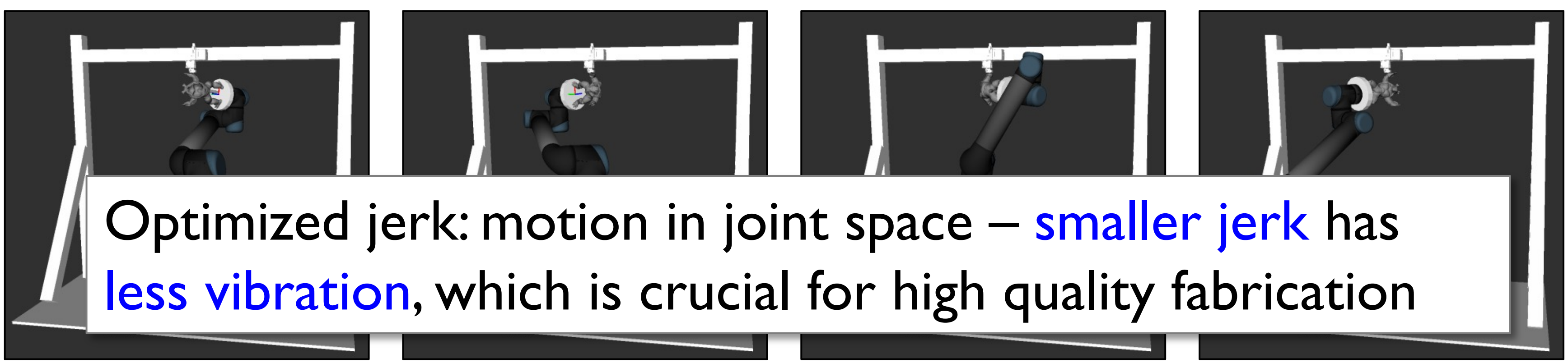

Optimized jerk: motion in joint space – smaller jerk has less vibration, which is crucial for high quality fabrication

Problem Statement

- Continuous Formulation (without hardware constraints):

$$\min_{\mathbf{q}(t)} \int \|\dddot{\mathbf{q}}\|_W \, dt$$
$$s.t. \quad \mathbf{x}(t) = f(\mathbf{q}(t)) \ \text{ and } \boxed{\Gamma(\mathbf{q}(t)) < 0}$$

Collision-free constraints specified by an indication function by its sign

  - Weighted norm: $\|\dddot{\mathbf{q}}\|_W = \sqrt{\mathbf{q}^T \mathbf{W} \mathbf{q}}$
  - Forward kinematic mapping: $f(\mathbf{q}) : \mathbf{q} \in \mathbb{R}^L \mapsto \mathbf{x} \in \mathbb{R}^5$

- Discrete Formulation (with hardware constraints):

$$\min_{\{\mathbf{q}_i\}} \mathbb{J} = \sum_{i=1}^{M} \|\dddot{\mathbf{q}}(t_i)\|_W^2$$
$$\begin{aligned} s.t. \quad & \mathbf{x}(t_i) = f(\mathbf{q}(t_i)) \quad (\forall i = 1, \ldots, M), \\ & \Gamma(\mathbf{q}(t_i)) < 0, \\ & \mathbf{q}_{\min} \le \mathbf{q}(t_i) \le \mathbf{q}_{\max}, \\ & |\dot{\mathbf{q}}(t_i)| \le \mathbf{v}_{\max}, \ |\ddot{\mathbf{q}}(t_i)| \le \mathbf{a}_{\max}, \ |\dddot{\mathbf{q}}(t_i)| \le \mathbf{j}_{\max}. \end{aligned}$$

  - Discrete-time constraints : $\mathbf{x}(t_i) = (\mathbf{p}_i, \hat{\mathbf{n}}_i) \qquad (\forall i = 1, \ldots, M)$

Experimental Results

Scenario 1

6DOF Setup

Example Tool-path

 C. Dai, S. Lefebvre, K.-M. Yu, J.M.P. Geraedts, and **C.C.L. Wang**, "Planning jerk-optimized trajectory with discrete-time constraints for redundant robots", *IEEE Transactions on Automation Science and Engineering*, vol.17, no.4, October 2020.

Outline

- Support-free volume printing by multi-axis motion
- Multi-axis filament alignment with controlled anisotropic strength
- Motion Planning:
  - Planning jerk-optimized trajectory for redundant robots (robotic arm + position table)
  - Singularity-aware motion planning for multi-axis additive manufacturing (x-, y-, z-movement + tilting head / table)

Higher Position Precision

Singularity Issues

Gaussian sphere

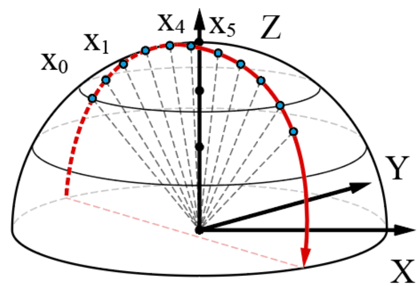

3D view

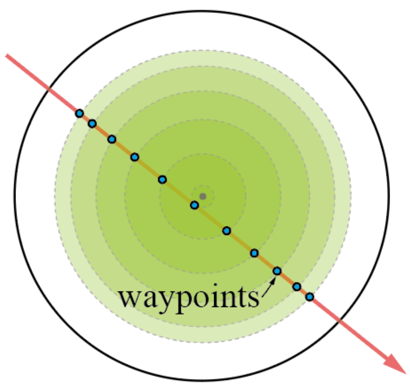

Top view

Cylinder coordinate

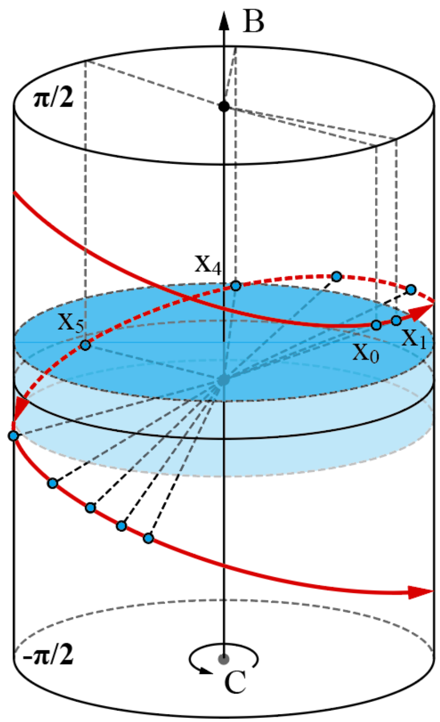

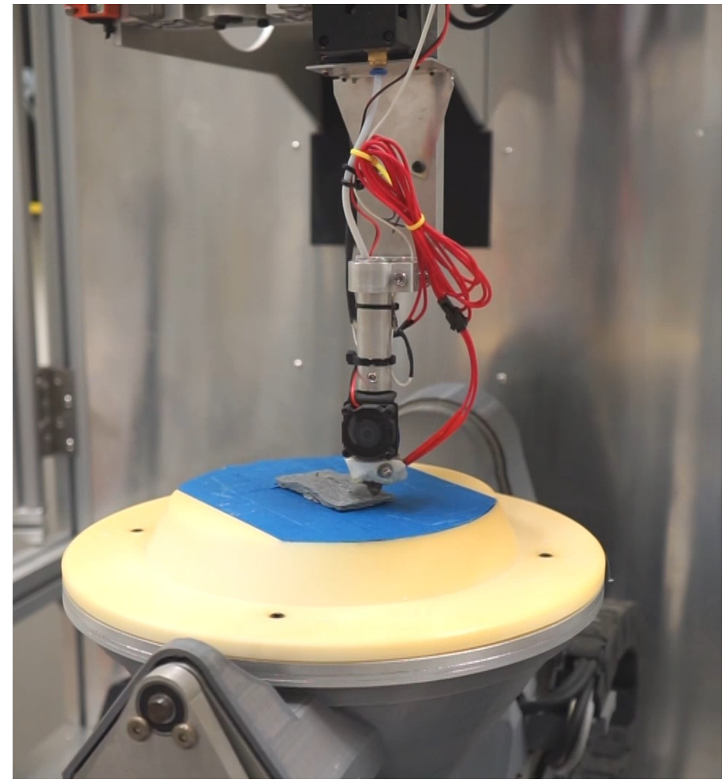

Nonlinear mapping in singular region

Uniformly sampled normal
in workpiece coordinate system

Non-uniform axis motion
in machine coordinate system

Three Types of Multi-Axis AM Machines

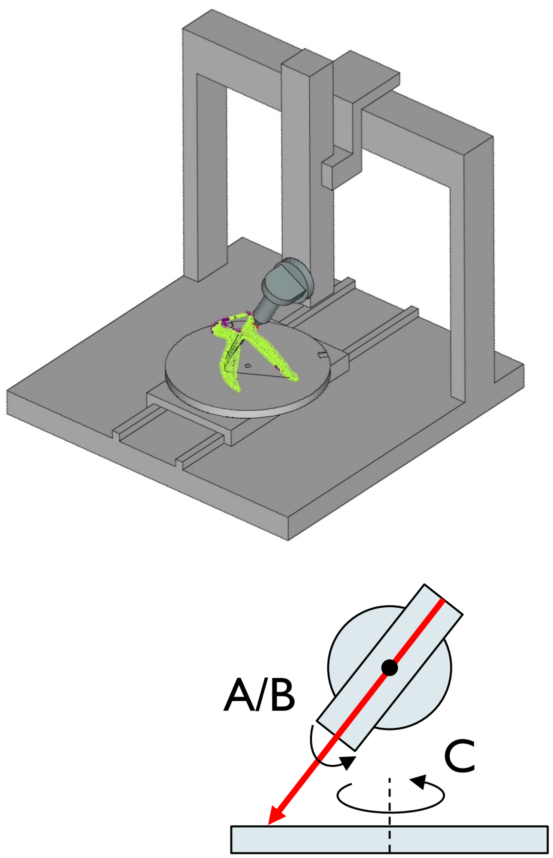

Rotational table & tilting head

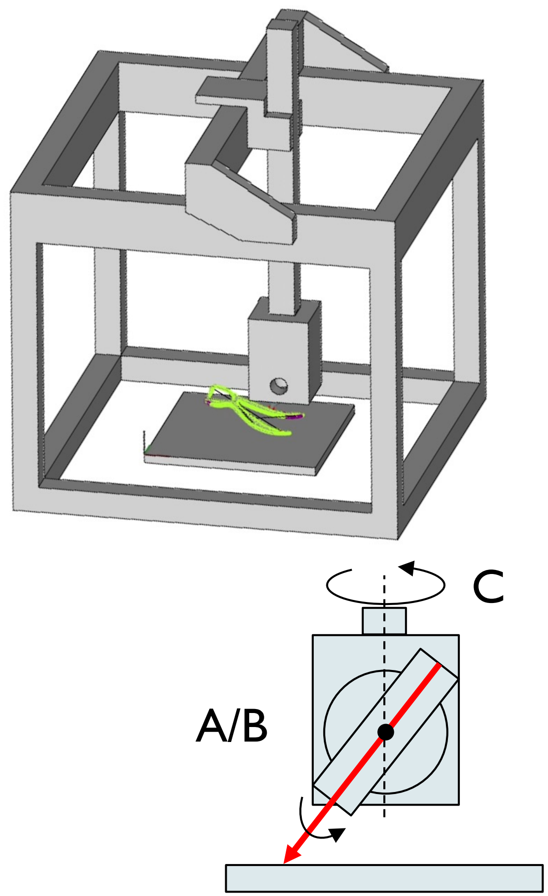

Rotational tilting head

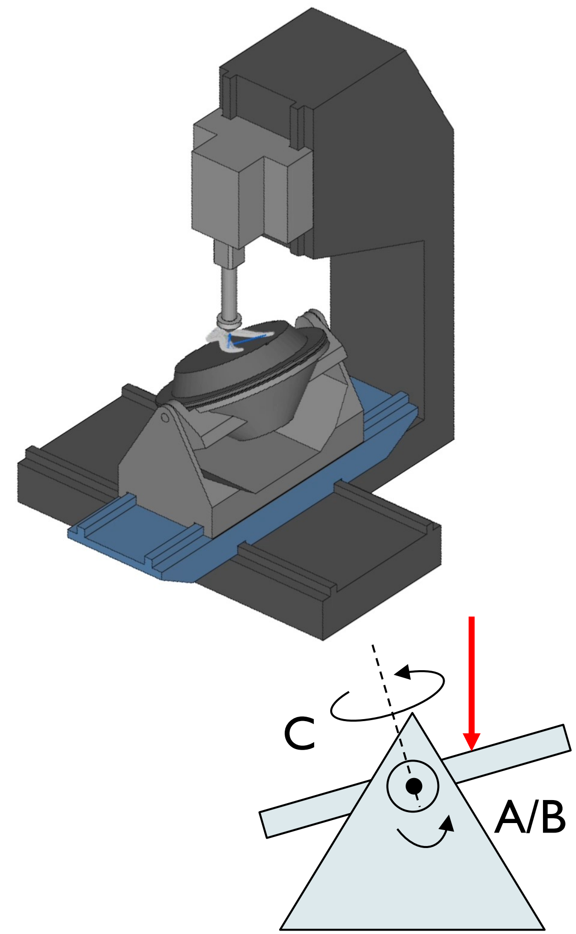

Rotational tilting table

Graph-Based Algorithm of Motion Planning

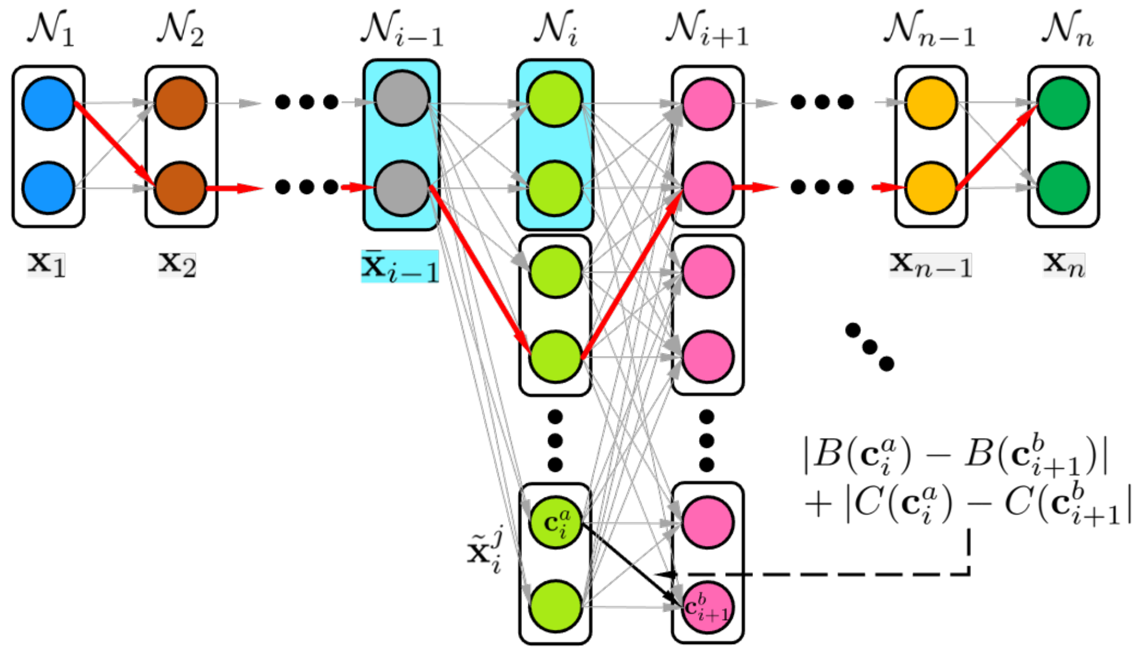

Step 1: Singular region processing (smooth in singular region)

Step 2: Generate collision-free variants (modify orientations)

Step 3: Find a shortest path that minimizes

$$J(\mathcal{T}) = \sum_i |B(\mathbf{c}_i^{\mathcal{T}_i}) - B(\mathbf{c}_{i+1}^{\mathcal{T}_{i+1}})| + |C(\mathbf{c}_i^{\mathcal{T}_i}) - C(\mathbf{c}_{i+1}^{\mathcal{T}_{i+1}})|$$

Experimental Results

Comparison

Motion

Before optimization

After optimization

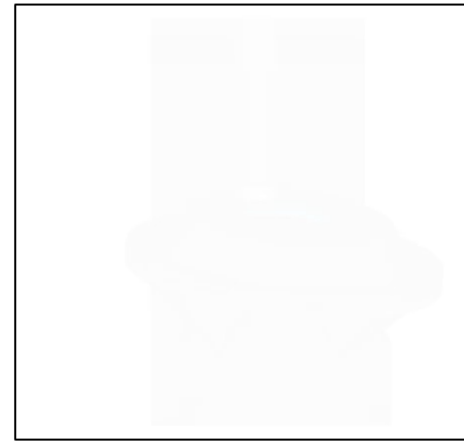

T. Zhang, X. Chen, G. Fang, Y. Tian, and **C.C.L. Wang**, "Singularity-aware motion planning for multi-axis additive manufacturing", IEEE Robotics and Automation Letters, 6(4). (Finalist of Best Student Paper Award – IEEE CASE 2021)

Conclusion Remarks

- A convex-front advancing method for support-free volume 3D printing – each model is peeled into curved layers can be collision-freely fabricated
- A field-based computational fabrication framework – the anisotropy of fused filaments is well controlled to reinforce the mechanical strength of 3D printed models
- A sampling based local filtering algorithm for planning discrete-time constrained trajectory on redundant robots
- A sampling based motion planning algorithm to generate a singularity-aware, smooth and collision-free motion

Impact of Developing "Real" 3D Printing

- Accumulating materials in space but not planar layers

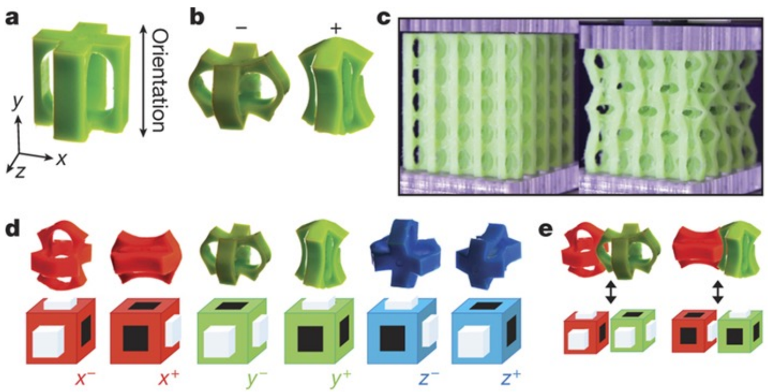

(a) Mechanical Meta-Materials [2] (Applied Physics)

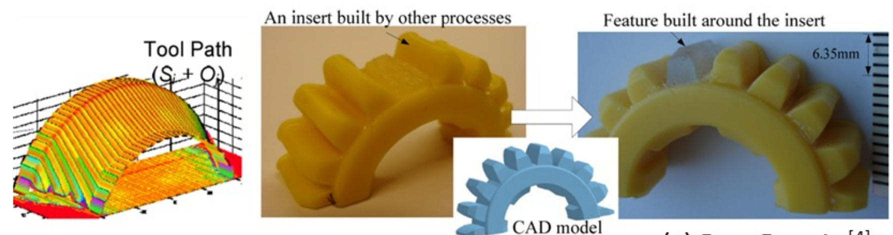

(c) Part Repair [4]

Multi-Axis Additive Manufacturing (Next Generation of 3D Printing)

Geometric Computing

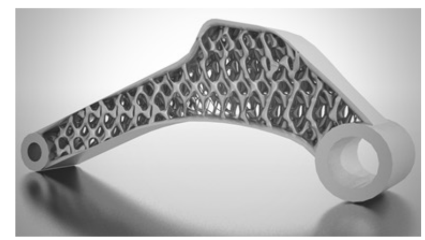

(d) Lightweight Structure (www.autodesk.com)

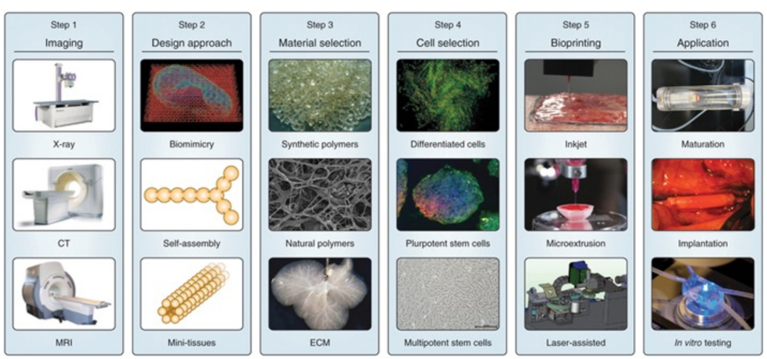

(b) Tissue Engineering [3] (Life Science)

(e) Large-Scale Construction [6]

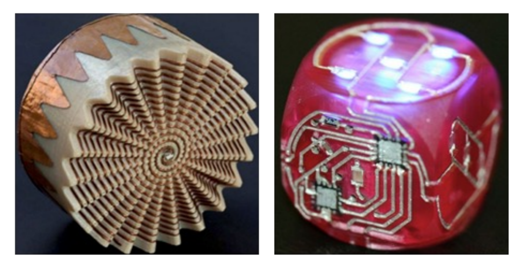

(f) Printing Electronics [8]

ZX. Zhao, Y. Pan, C. Zhou, Y. Chen, and **C.C.L. Wang**, "An integrated CNC accumulation system for automatic building-around-inserts", Journal of Manufacturing Processes, vol.15, no.4, 2013. (**NAMRI/SME Outstanding Paper Award**)

3D Printing Continuous Reinforced Thermoplastic Composites: Adaptive Toolpaths

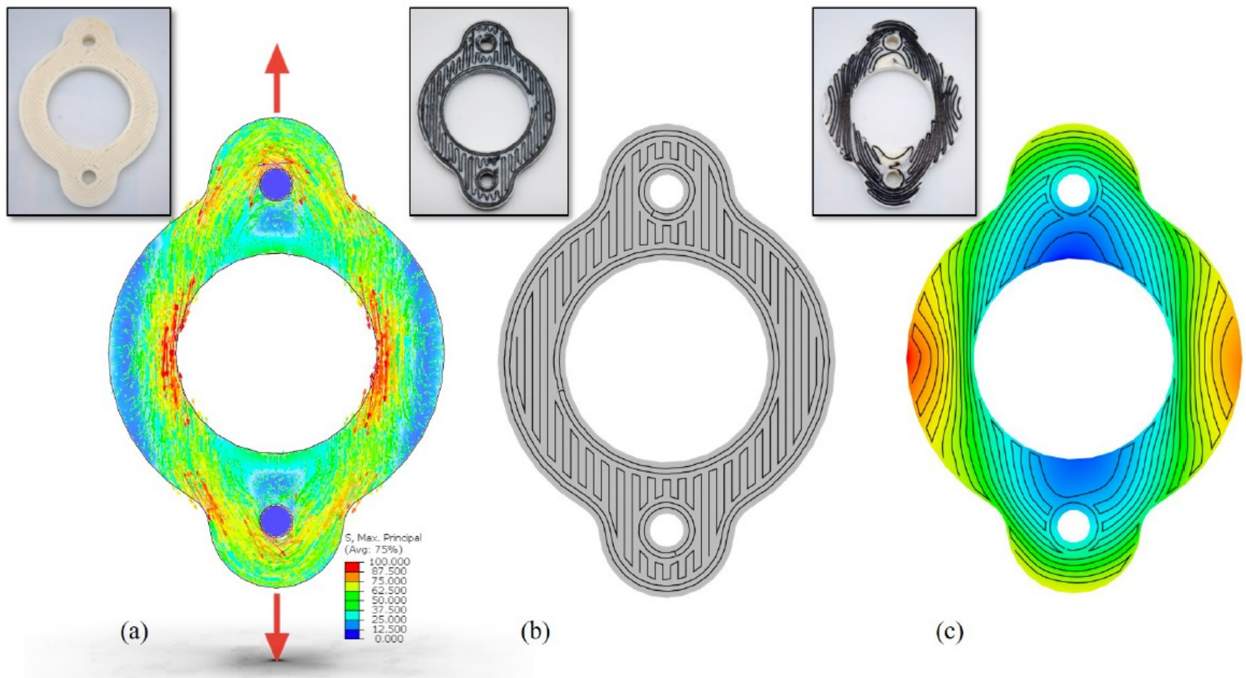

Breaking force: 171.4%
Stiffness: 150.2%

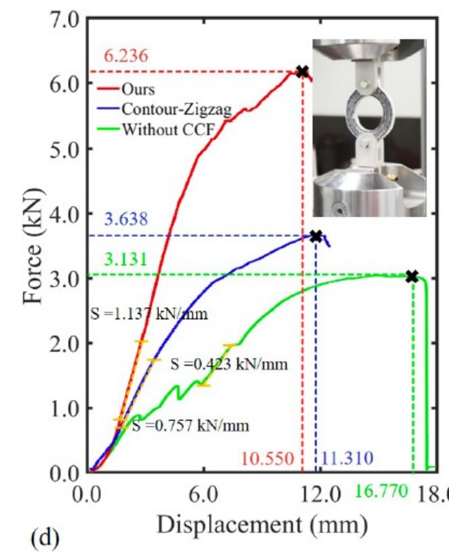

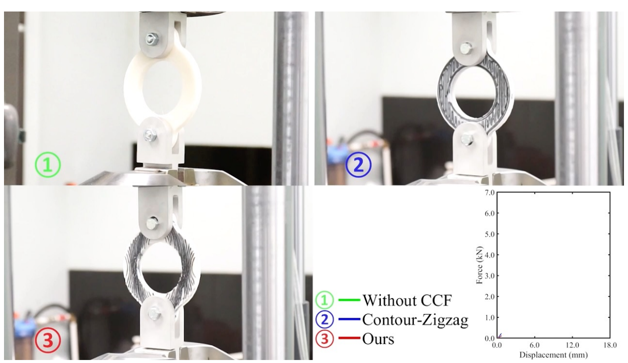

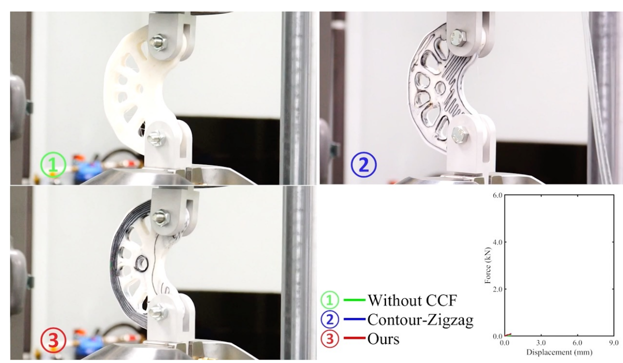

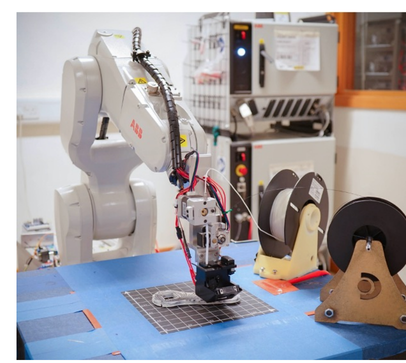

X. Chen, G. Fang, W.H. Liao, and **C.C.L. Wang**, "Field-based toolpath generation for 3D printing continuous fibre reinforced thermoplastic composites", Additive Manufacturing, vol.49, 102470 (13 pages), January 2022.

Robot-Based Bioprinting for Bioactive Artificial Blood Vessel & Cardiac Tissue

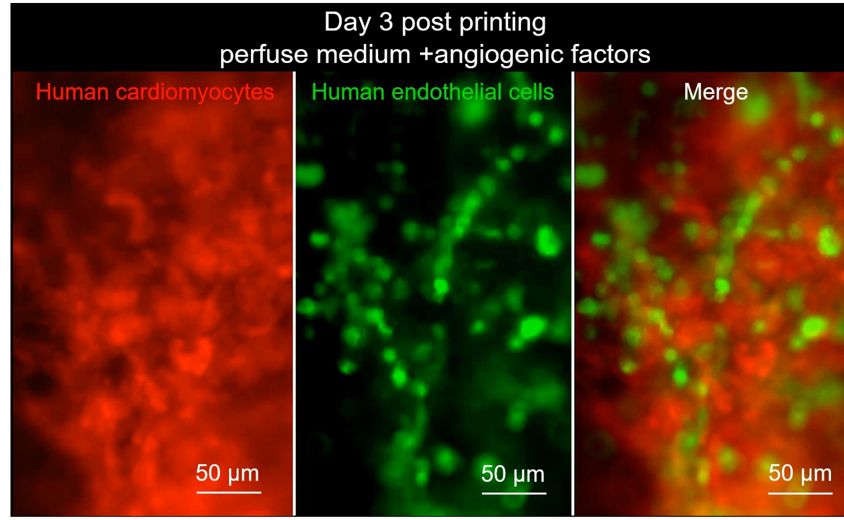

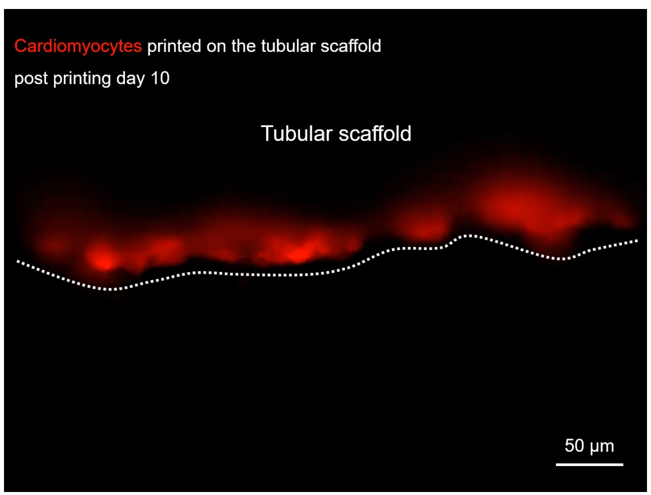

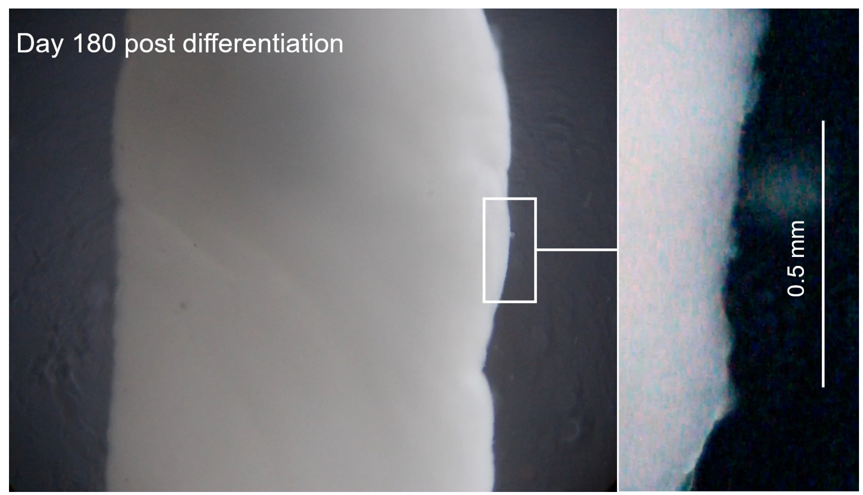

 Z. Zhang, C. Wu, C. Dai, Q. Shi, G. Fang, D. Xie, Y.J. Liu, **C.C.L. Wang**, and X.J. Wang, "A multi-axis robot-based bioprinting platform for bioactive artificial blood vessel and cardiac tissue fabrication", Bioactive Materials, vol.18, pp.138-150, 2022.

Acknowledgment

- PhD Students
  - Chengkai Dai (TU Delft)
  - Guoxin Fang (TU Delft / UoM)
  - Tianyu Zhang (U. Manchester)
  - Yingjun Tian (U. Manchester)
  - Neelotpal Dutta (U. Manchester)
  - Yuming Huang (U. Manchester)
- Collaborators
  - Sylvain Lefebvre (INRIA)
  - Jo Geraedts (TU Delft)
  - Kai-Min Yu (HK PolyU)
  - Yong-Jin Liu (Tsinghua)
  - Xiu-Jie Wang (CAS)
  - Zichun Zhong (Wayne State)
- Funding Sources
  - MACE Dept. @ U Manchester
  - IDE Faculty @ TU Delft
  - MAE Dept. @ CUHK
  - Hong Kong RGC General Research Fund (GRF)
  - China Scholarship Council

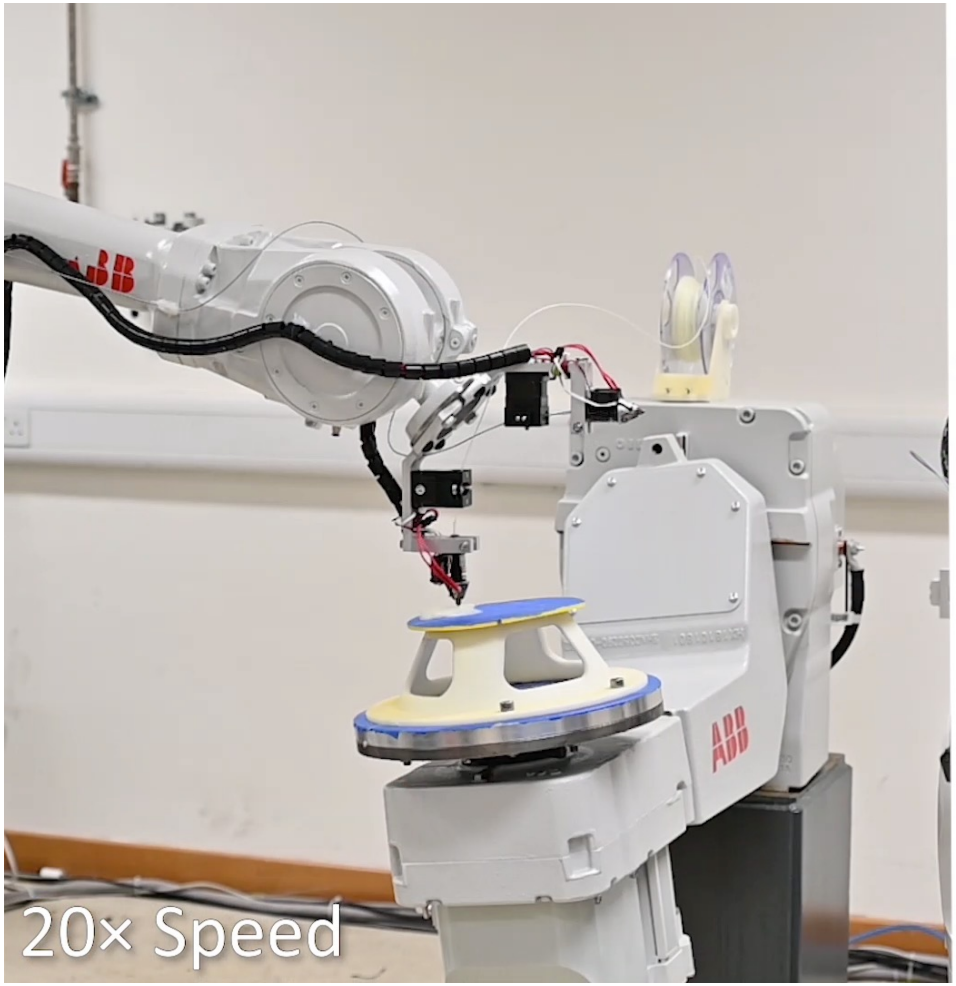

Physical fabrication realized on a robotic platform with 8-DOFs

Charlie C. L. Wang
Dept. of Mechanical, Aerospace & Civil Eng.
The University of Manchester
E-mail: changling.wang@manchester.ac.uk

Toolpath Gen.

Motion Planning